J Multidisciplinary Scientific Journal

MDPI

Article

Adsorptive and Coagulative Removal of Trace Metals from Water Using Surface Modified Sawdust-Based Cellulose Nanocrystals

Opeyemi A. Oyewo [1,*], Sam Ramaila [1], Lydia Mavuru [1], Taile Leswifi [2] and Maurice S. Onyango [3]

[1] Department of Science and Technology Education, University of Johannesburg, Johannesburg 2092, South Africa; samr@uj.ac.za (S.R.); lydiam@uj.ac.za (L.M.)
[2] Department of Chemical and Civil Engineering, University of South Africa, Florida Campus, Roodepoort 1709, South Africa; leswity@unisa.ac.za
[3] Department of Chemical, Metallurgical and Materials Engineering, Tshwane University of Technology, Pretoria 0001, South Africa; onyangoms@tut.ac.za
* Correspondence: Atiba.opeyemi@gmail.com; Tel.: +27-720-200-084

Abstract: The presence of toxic metals in surface and natural waters, even at trace levels, poses a great danger to humans and the ecosystem. Although the combination of adsorption and coagulation techniques has the potential to eradicate this problem, the use of inappropriate media remains a major drawback. This study reports on the application of $NaNO_2/NaHCO_3$ modified sawdust-based cellulose nanocrystals (MCNC) as both coagulant and adsorbent for the removal of Cu, Fe and Pb from aqueous solution. The surface modified coagulants, prepared by electrostatic interactions, were characterized using Fourier transform infrared, X-ray diffraction (XRD), and scanning electron microscopy/energy-dispersive spectrometry (SEM/EDS). The amount of coagulated/adsorbed trace metals was then analysed using inductively coupled plasma atomic emission spectroscopy (ICP-AES). SEM analysis revealed the patchy and distributed floccules on Fe-flocs, which was an indication of multiple mechanisms responsible for Fe removal onto MCNC. A shift in the peak position attributed to $C_2H_{192}N_{64}O_{16}$ from 2θ = 30 to 24.5° occurred in the XRD pattern of both Pb- and Cu-flocs. Different process variables, including initial metal ions concentration (10–200 mg/L), solution pH (2–10), and temperature (25–45 °C) were studied in order to investigate how they affect the reaction process. Both Cu and Pb adsorption followed the Langmuir isotherm with a maximum adsorption capacity of 111.1 and 2.82 mg/g, respectively, whereas the adsorption of Fe was suggestive of a multilayer adsorption process; however, Fe Langmuir maximum adsorption capacity was found to be 81.96 mg/g. The sequence of trace metals removal followed the order: Cu > Fe > Pb. The utilization of this product in different water matrices is an effective way to establish their robustness.

Keywords: adsorption; coagulation; cellulose nanocrystals; sawdust; trace metals

Citation: Oyewo, O.A.; Ramaila, S.; Mavuru, L.; Leswifi, T.; Onyango, M.S. Adsorptive and Coagulative Removal of Trace Metals from Water Using Surface Modified Sawdust-Based Cellulose Nanocrystals. *J* **2021**, *4*, 193–205. https://doi.org/10.3390/j4020016

Academic Editor: Raed Abu-Reziq

Received: 28 April 2021
Accepted: 8 June 2021
Published: 14 June 2021

1. Introduction

A significant amount of heavy metals from industrial effluents ends up in the environment and adversely affects the quality of water [1]. Some major industrial sources of toxic metals include surface treatment processes and coating of industrial products involving the use of metals such as Cu, Fe, Ni and Pb [2]. Heavy metals are non-biodegradable, and thus remain in both the environment and biological systems for a long period. In addition, traces of heavy metals could slowly accumulate in the human body over a long period of time [3,4], thereby exerting negative health effects on human tissues. Although the use of these metals in the industries is in high demand due to their various applications and benefits, their prevention from reaching downstream processes and subsequently ending up in the receiving waters remains a major challenge. For example, the consumption of copper within the allowable limit could improve the human immune system, aid digestion, and

enhance wound healing [5]. However, the presence of copper in drinking water beyond the allowable concentration (0.1 mg/L) is highly toxic to the human system and poses a great health danger [6,7]. In addition, Cu is toxic to monogastric animals when ingested in quantities that are 40 to 135 times greater than their allowable requirements. Iron is another toxic metal whose high concentration in drinking water could also be detrimental to human health. Although adults could be protected from slightly high concentrations of iron, children within 1 to 2 years of age are particularly vulnerable to iron toxicity [8]. Lead, unlike other heavy metals, has no health benefits to humans even at trace levels. It is extremely toxic and mainly targets human organs such as bones, the brain, blood, kidneys, and the thyroid glands [9,10].

As a consequence of the potential of these metals to cause harm [11], there has been a global increase in awareness and tightening in the regulations on the disposal of heavy metal-containing effluents. Hence, the removal of metals from wastewater to a maximum allowable concentration has been recommended by different agencies such as the European Union and the Water Framework Directive (WFD) (2000/60/EC), which has recently specified bioavailability-based standards for Pb, Fe and Cu, classified as priority hazardous substances. Bioavailability-based standards have also been specified for Zn, which is classified as specific pollutants under the WFD in the United Kingdom [12].

Thus, to ensure compliance with regulatory standards, it is important to explore different treatment technologies in order to enhance trace metal removal from wastewater [13]. Conventional processes used for wastewater treatment could be divided into two main phases: (1) generation of suspended solids from colloidal and dissolved solids by physical, chemical and biological means in addition to the already existing suspended solids; (2) separation of suspended solids by chemical and mechanical methods including sedimentation, flotation and filtration [14]. Despite the constant development of new and improved treatment processes, coagulation/flocculation (CF) remains an important process for wastewater treatment, owing to its simplicity in design and operation, low energy consumption and versatility [13,15]. In addition, the use of CF as a treatment option is due to the fact that CF could be operated as a primary, secondary or tertiary treatment technique and also intermittently [13]. The coagulation/flocculation process mainly involves the addition of compounds that promote the clumping of fines into larger floc so that they can be more easily separated from the water [16]. However, the main mechanisms that usually occur and are mostly responsible for the success of any coagulation of metals are adsorption and co-precipitation. Hence, the adsorption process is a surface phenomenon, whereby the substance gets adsorbed on the surface, and co-precipitation only occurs with the help of a base in a solvent [17]. Therefore, it is hereby speculated that the adsorption mechanism is often responsible for the coagulation of toxic metal ions from water. However, the choice of coagulant used and water matrix to be treated contribute to the metal removal mechanism.

Chemically synthesized or polymer-based coagulants have proven to be highly efficient in trace metal coagulation. However, their presence in the environment and in human system has been specifically linked to Alzheimer and dementia disorders [18,19]. The severity of their adverse effect on the human system has inspired further investigation into the generation of highly efficient and environmentally-friendly coagulants that could serve as a good replacement for toxic coagulants. In our previous studies, a highly efficient cellulose nanocrystals-based coagulant and its performances in Ni and Cd removal from water was presented. However, the study of the performance of any green materials in different water matrices is necessary in order to confirm its robustness.

Consequently, in our study a non-toxic, highly efficient and cheap coagulant has been utilized for the removal of toxic trace metals from water using both coagulation and adsorption approaches. The performance of the coagulant was studied using a jar test apparatus in which the coagulant dose, metal ions concentration and solution pH were varied. The capacities of the coagulant and the mechanism governing the removal of the three target ions (Cu, Pb and Fe) were investigated using adsorption techniques. Although the details of the physicochemical properties of the pristine and modified CNC, such as functional groups,

structures and surface charge, have been previously reported, the current study focuses on the properties of the floccules obtained in the subsequent trace metal ions removal.

2. Materials and Methods

2.1. Materials

All chemicals used were of analytical grade. Cellulose nanocrystals (CNC) were supplied by the Council for the Scientific and Industrial Research (CSIR), Durban, South Africa [20]. The pH of the solution was adjusted with 0.1 mol/L NaOH and 0.1 mol/L HCl, and other chemicals such as $NaNO_2$, $NaHCO_3$, HNO_3, $CuSO_4$, $PbSO_4$, and $Fe(NO_3)_3$ were obtained from Sigma-Aldrich, Pretoria, South Africa.

2.2. Methods

2.2.1. Surface Modification of Cellulose Nanocrystals (CNC)

The extraction process and the details of the synthesis route of utilized cellulose nanocrystal coagulant have been reported elsewhere [21]. Pristine CNC was modified in aqueous phase using $NaNO_2/NaHCO_3$. The first stage of modification involved the addition of 0.025 mol/L of $NaNO_2$ to a reactor containing raw CNC under vigorous stirring at 75 °C for 1 h. Afterwards, 5 mL of nitric acid was added to the mixture as the stirring continued for a further 24 h. The product obtained was separated by centrifugation at 60 rpm for 40 min, and was then thoroughly washed to remove the unreacted materials until the pH was near neutral at > 6.5. Sodium nitrite was added to the mixture to achieve the deprotonation of the CNC and the formation of the sodium salt on the surface (Figure 1a). In the second stage, conversion of the carboxyl groups (COOH) to carboxylate groups (COONa) occurred by treating the CNC suspensions with 0.025 mol/L $NaHCO_3$ solution at room temperature for 30 min. The MCNC was also rinsed with deionised water until the pH of the material was around 7 (Figure 1b). The addition of sodium bicarbonate introduced the carbonyl group, which underwent bond opening to yield anionic oxygen groups on the surface of the material.

2.2.2. Characterization of Synthesized and Spent Cellulose Nanocrystals Coagulants

Details of the characterization of raw CNC and modified CNC have been extensively reported in our previous study [21]. Nevertheless, the characterization of raw CNC, modified CNC and the flocs formed after coagulation of the three trace metals (Cu, Pb and Fe) are also discussed in this study. All of the CNC samples were air dried for 48 h to get rid of the remaining moisture content prior to any characterization analysis. Fourier transform infrared (FT-IR) spectroscopy, scanning electron microscopy (SEM), and X-ray diffraction analytical techniques were used. The FT-IR spectroscopic analysis was performed using a Perkin Elmer Spectrum 100 spectrometer. The morphology and composition of the materials were characterized by SEM/EDS using a JEOL JSM-7600F field emission scanning emission microscope (FESEM), running at 2 kV accelerating voltage. The crystallinity was analysed using an X-ray diffractometer (XRD) (PANalytical Empyrean) under the following conditions: 45 mA, 40 kV and monochromatic Cu Kα radiation (λ = 0.15406 nm) over a scan range of 2θ = 5.0–90.0°.

2.2.3. Coagulation-Flocculation Studies

The CF studies were conducted in conventional jar test stirrers, which allowed six beakers to be agitated simultaneously. Each jar test consisted of a batch experiment involving rapid mixing, slow mixing and sedimentation. Each of the trace metals were investigated separately. A 1 L beaker was filled with 500 mL of trace metals-laden waters, agitated at the preselected intensity of rapid mixing (200 RPM for 2 min). Afterwards, the preselected intensity of slow mixing (60 RPM for 20 min) was immediately established. The beakers were removed from the floc illuminator for a 30 min sedimentation phase. Subsequently, supernatants were withdrawn from about 25 mm below the surface using a syringe and analysed using an inductive coupled plasma atomic emission spectrometer

(ICP-AES, 9000, Shimadzu, Johannesburg, South Africa) to confirm the residual metal concentration. Each coagulation test was run in triplicate and the result reported is the arithmetic average result of the three, and the standard deviation was about 0.00002 in all cases. The flocs were freeze-dried for further characterization. In optimising the solution pH parameters, a set of experiments was run without coagulant added for each of the trace metals; it was therefore treated by changes in pH and stirring only, which serve as a pH control experiment.

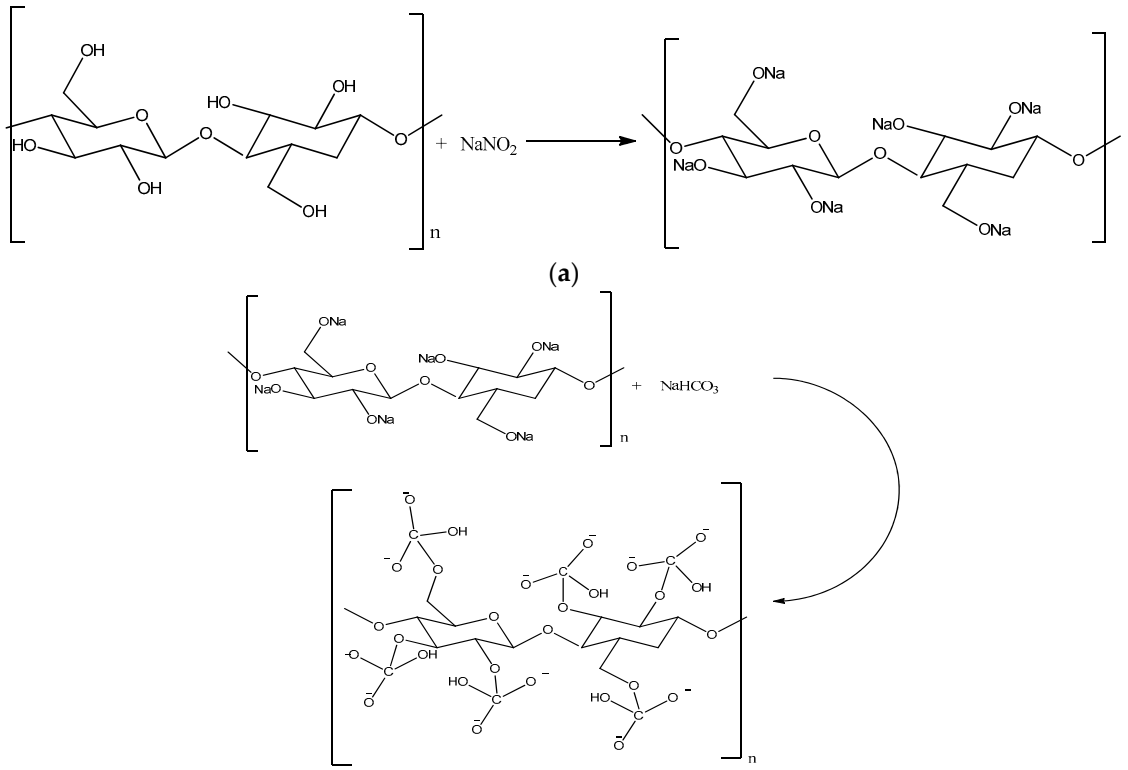

Figure 1. Proposed reaction scheme for the (**a**) modification of CNC with sodium nitrite ($NaNO_2$), and (**b**) conversion of the sodium salt of cellulose to carboxylate anion across the surface of the modified material. Reprinted from [21]. Copyright (2019), with permission from Elsevier.

2.2.4. Adsorption Studies

The adsorption process was studied by varying the initial concentration of the Cu/Pb/Fe and reaction temperature in a batch system. Initially, the effect of solution pH and optimum dosage were explored between pH 2 and 10 and 5 and 25 mg/L, respectively, using coagulation mode. pH 7 was considered to be optimum and it was used for the subsequent adsorption process. It was also confirmed in the coagulation experiment that 5 mg/L MCNC was more favourable for coagulation of all the trace metals in 500 mL of water, which is equal to 0.5 mg/L MCNC for 50 mL of trace metals-laden water treatment. Therefore, 0.5 mg/L of MCNC was added to the prepared 50 mL solution of different concentrations of Pb/Cu/Fe separately in 100 mL plastic bottles under different temperatures in order to determine the effect of temperature and obtain the isothermic data. The bottles were placed in a thermostatic bath shaker running at a speed of 200 rpm for 24 h. The samples were then filtered using Whatman filter paper No. 42 and the filtrates were analysed by ICP-AES to determine the residual concentration of the trace metals.

3. Results and Discussion

3.1. Characterization Results

3.1.1. Fourier Transform Infrared (FT-IR) Spectroscopy

The details of the functional groups in raw CNC, MCNC, Pb-flocs, Cu-flocs and Fe-flocs were studied using FT-IR spectroscopy. The spectra were recorded in the range of 400 to 4000 cm^{-1} as presented in Figure 2. The bands between 3286 and 3486 cm^{-1} in all of the samples were attributed to the O-H stretching vibration. A reduction in the intensity of these bands occurred upon modification, which indicated the participation of the oxygen atom in the bonding interaction with the $NaNO_2/NaHCO_3$, thereby resulting in the weakening of the O-H bond strength. The intensity of the band at 1435 cm^{-1}, ascribed to the carbonyl group, increased after incorporating the $NaNO_2/NaHCO_3$ and this was indicative of an enhancement in the crystallinity of this media upon functionalization [22]. The disappearance of the band attributed to the carbonyl group around 1435 cm^{-1} indicated the participation of the oxygen of this group in a covalent bonding to the metal ions of Cu, Fe and Pb. The appearance of the C-O band around 1150 cm^{-1} in the spectra of spent materials (floccules) is a consequence of this bonding interaction, and confirmed the participation of the carbonyl group in the removal of trace metals from the water [23]. The band around 1000 cm^{-1} was ascribed to the stretching vibration of C-O, and the additional band on MCNC at 700 cm^{-1} was due to the symmetric bending mode of $NaNO_2$ [24]. The vibrational band around 2920 cm^{-1}, which was the C-H vibration of sp^3 hybridized carbon, disappeared upon modification [21]. Surprisingly, this band reappeared on the spectrum of Pb-flocs, suggesting that this functional group has no impact on the coagulation of Pb as it does for other metals. Similar results were reported on the coagulation of heavy metals using another coagulant [25,26].

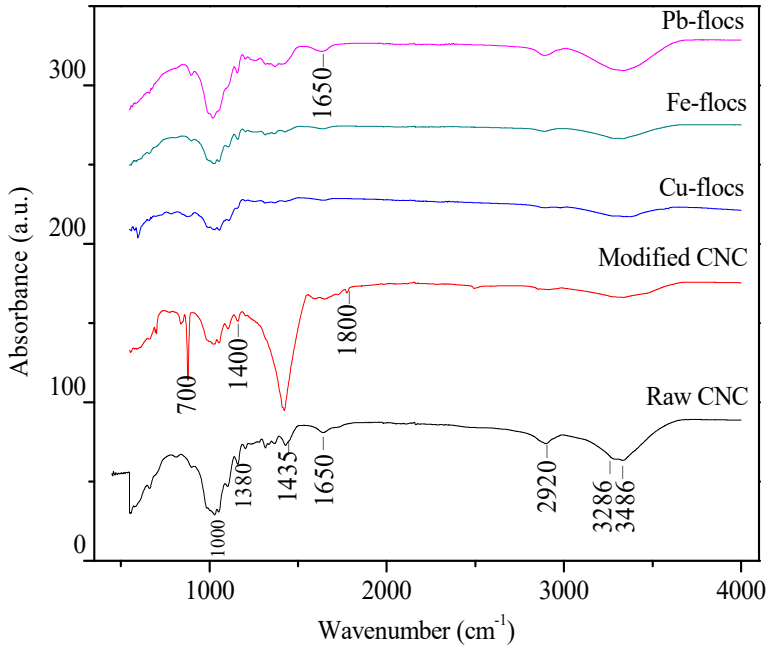

Figure 2. FT-IR Spectra of Raw CNC (unmodified), $NaNO_2/NaHCO_3$ modified CNC, Cu-flocs, Fe-flocs and Pb-flocs.

3.1.2. Scanning Electron Microscopy Analysis

The microscopic properties of pristine CNC, MCNC and floccules obtained from Cu/Pb/Fe is presented in Figure 3a–e. The micrograph of pristine CNC displayed a plane surface with slightly granular particles and fibres (Figure 3a); the granular particles became more pronounced in the MCNC surface and the pores were distributed across the samples with a homogenous rough surface (insert Figure 3b). The change in morphological

properties upon coagulation of the toxic metals can be noticed in Figure 3c–e. The clustered form of floccules observed during Pb coagulation (Figure 3c) suggests that the reaction occurred at a specific homogenous site on the surface of the MCNC. However, the floccules formed in the coagulation of Cu were well distributed across the surface of the MCNC (insert Figure 3d). The patchy and poorly distributed flocs observed in the Fe coagulation suggests dual mechanisms in the process (insert Figure 3e) [27].

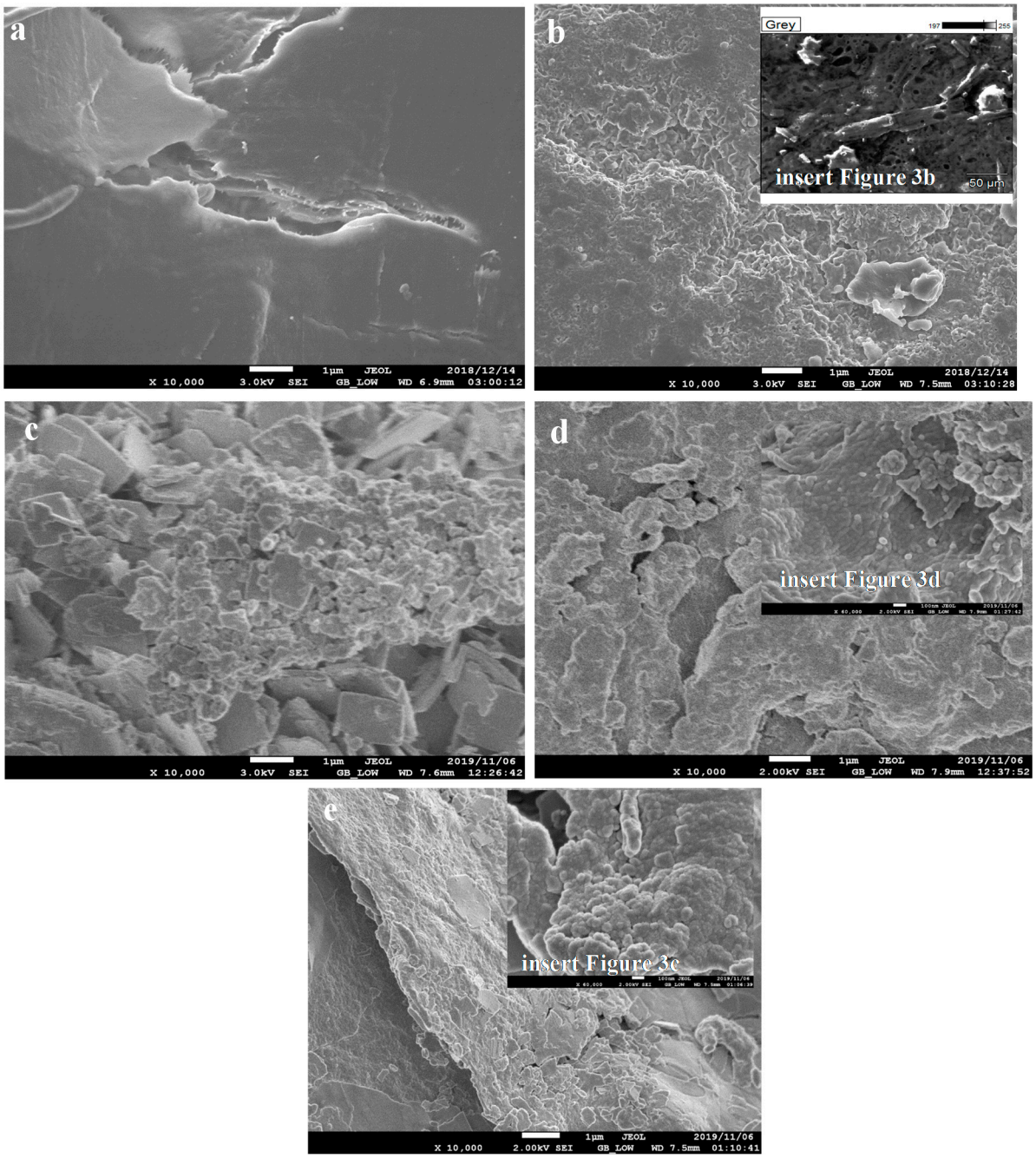

Figure 3. SEM images of: (**a**) Raw CNC (unmodified) (**b**) $NaNO_2/NaHCO_3$ modified CNC, insert Figure 3b: MCNC ×50 µ (**c**) Pb-flocs (**d**) Cu-flocs, insert Figure 3d: Cu-flocs magnification ×60,000 (**e**) Fe-flocs, insert Figure 3e: Fe-flocs magnification ×60,000.

The elemental composition of the MCNC, Cu-flocs, Fe-flocs and Pb-flocs is summarized in Table 1. As expected, the CNC materials mainly possessed carbon and oxygen. The observed high percentage of Na in MCNC was due to the functionalization of CNC with

sodium salt. The presence of Cu, Fe and Pb on their respective spent materials indicated the success of adsorption/coagulation of these trace toxic metals.

Table 1. EDS analysis of MCNC, and floccules formed during the coagulation process.

Element wt.%	MCNC	Cu-flocs	Fe-flocs	Pb-flocs
C	20.21	45.24	46.92	39.9
O	33.15	37.51	33.27	40.5
Na	24.25	2.1	-	-
Mg	0.04	0.03	-	-
Al	11.09	1.72	0.75	0.14
Si	3.06	0.03	0.69	
S	7.30	1.28	4.4	2.5
Pb	-	-	-	16.34
Cl	0.83	-	-	
Fe	-	-	13.92	-
Cu	-	12.09	-	-
K	0.03	-	0.02	0.62
Ca	0.04	-	0.03	-
Total	100	100	100	100

3.1.3. X-ray Diffraction (XRD) Analysis

The X-ray diffraction patterns of the Pristine CNC, MCNC, Cu-flocs, Fe-flocs and Pb-flocs displayed peaks associated with the 1α and 1β phases of crystalline cellulose ($C_{60}H_{88}O_8$ and $C_2H_{192}N_{64}O_{16}$) [19,20] as presented in Figure 4. Peaks at 2θ = 45°, 30.1° and 28.6° in the diffraction patterns of MCNC and the metal floccules were due to the presence of crystalline sodium nitrite and sodium carbonate in these samples [28], suggesting very strong interactions between sodium units and the cellulose structure [14]. Additional phases ($C_{36}H_{36}N_4O_8$, $Ca_{12}Al_{24}O_{48}$ and $C_{16}H_{32}O_4$) were also noticed upon modification of CNC, which confirmed the presence of modifiers within the lattice of CNC. A shift in the position of the peak associated with $C_2H_{192}N_{64}O_{16}$ at 2θ = 30 to 24.5° was observed in the diffraction patterns of Pb-flocs and Cu-flocs, but complete disappearance occurred in the floccules obtained from Fe coagulation. This suggested a strong chemical interaction involving $C_2H_{192}N_{64}O_{16}$ and trace metals in the solution. In addition, the disappearance of peaks due to $Ca_4Al_8Si_{12}O_{52}H_{24}$ from the modified CNC sample upon coagulation of Cu, Fe and Pb suggested the involvement of these phases in the metal coagulation process [21]. Similar results have been reported in the literature [29,30]

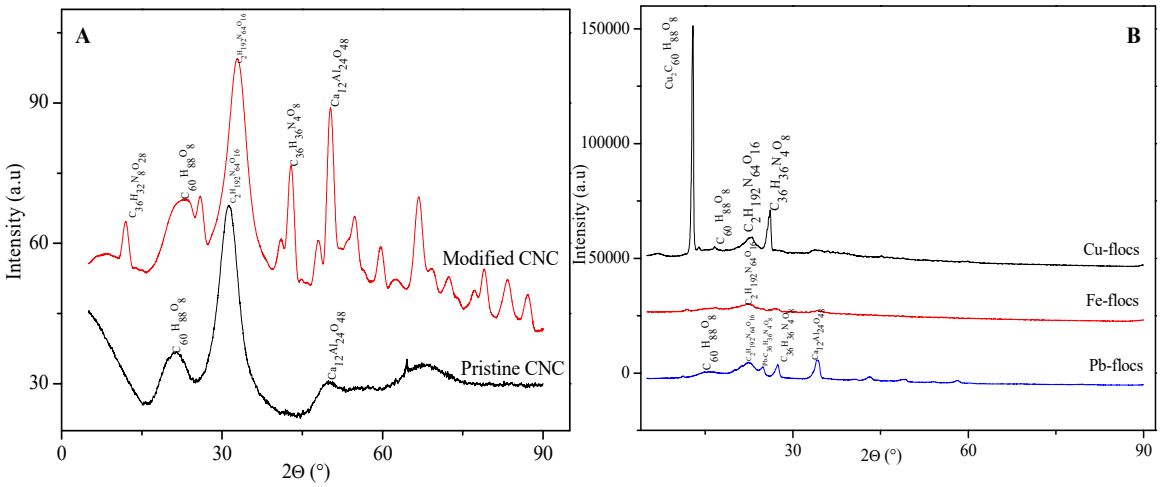

Figure 4. X-ray diffraction patterns of pristine CNC, MCNC and metal floccules.

3.2. Coagulation Results

3.2.1. Effect of Metals Solution pH

Coagulation of the trace metals from aqueous solutions using the pristine CNC and MCNC in a pH range of 2 to 8 are presented in Figure 5a–c. Control experiments were first conducted to confirm the precipitation of these metals before introducing the coagulant. It is reported that the rate of precipitation increased with an increase in dissolution rate as the solution became more concentrated [31]. Therefore, little or no reduction in the concentration of Cu and Pb were observed in the acidic medium up to pH 7.20; however, the removal efficiencies obtained from pH 7.20 to 10 might be due to dual mechanisms suggested to be precipitation and adsorption in Figure 5a,b. An increase in the reduction of Fe was observed as the pH increased, which was an indication of a precipitation between pH 3 and 10 (Figure 5c) [32]. Apparently, the pH of the media strongly influences the removal efficiency of the metals, and the optimum pH 7 is appropriate for the treatment of water fit for consumption. In general, the modified CNC was observed to perform better than pristine CNC. Although about 44% removal of Fe occurred via precipitation, prior to coagulant dosage (Figure 5c), a complete removal of this trace metal was noticed upon the addition of MCNC. This could be attributed to another type of mechanism, which most likely would be the adsorption process. There are three proposed steps in the adsorption process of these trace metals: (1) migration of ions onto the surface, (2) deprotonation or dissociation of an aqueous complex of Pb/Cu/Fe and (3) surface complexation [33]. Consequently, the adsorption process was investigated in order to confirm the in-depth mechanism that occurred in the removal of these trace metals. In our previous study [21], the magnitude of negative charge of the coagulant was reported upon modification, and this might also reduce the repulsive forces between CNC particles, thereby enhancing the uptake of the positively charged Cu, Pb and Fe.

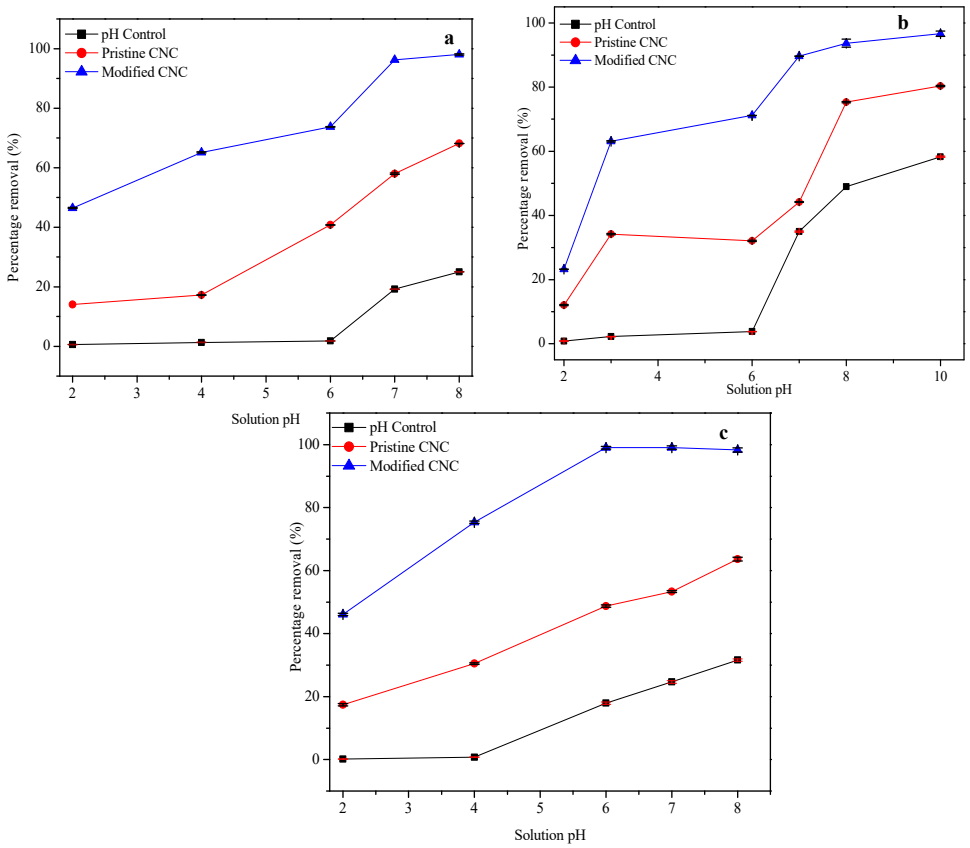

Figure 5. Effects of solution pH on trace metals removal from aqueous solution: (**a**) Cu (**b**) Fe (**c**) Pb (coagulant dosage 5 mg/L, initial concentration 20 mg/L, volume 1000 mL).

The solubility in the aqueous systems was reduced due to the loss of sodium ions during modification (Figure 1). In addition, the presence of the anions in the solution increased the exposure of MCNC to the complexation reaction with Cu/Fe/Pb through the coordinate bond as presented in Figure 6. The trace metals were then precipitated out and separated by centrifugation and filtration [21].

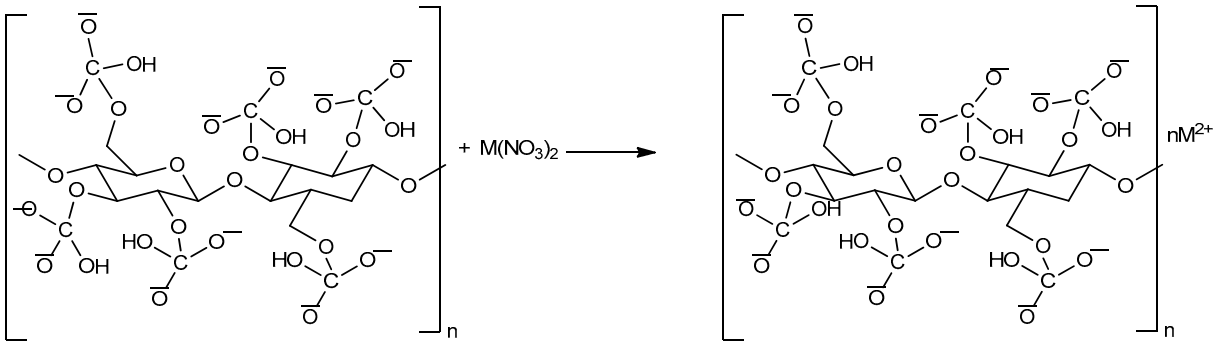

Figure 6. Proposed reaction scheme for the coagulation of Cu/Pb/Fe on to MCNC.

3.2.2. Effect of Coagulant Dosage

The coagulant dose was varied from 0.5 to 25 mg/L, and Figure 7 presents the trace metals removal efficiency (%) as a function of coagulant dosage (mg). An increase in the removal efficiency of Fe and Pb was observed, which corresponded to an increase in coagulation because of increased availability of active sites. There was an increase in the removal of Fe and Cu compared to Pb, which confirmed that Fe and Cu ions have higher affinity for the functional groups embedded in MCNC [21]. The uptake efficiency of Cu increased with the increase in coagulant dosage from 0.5 to 5 mg/L. However, a drastic decrease in the removal of Cu ions could be noticed after increasing the dosing from 10 up to 25 mg/L. This is because the optimum dosage for the removal of trace Cu in aqueous solutions is 5 mg/L. Therefore, very little coagulant was used per cubic meter of Cu-laden water, which is one of the major advantage of using the coagulation process in water treatment. In addition, it must be noted that an overdose of coagulant does not enhance Cu ion removal from water but, by contrast, results in decreased Cu removal efficiency. This is because MCNC has reached an equilibrium for Cu ions in the solution, and therefore, the desorption of initially adsorbed Cu ions is suspected at high coagulant doses due to continuous stirring. A similar observation was reported in our previous study [28] and other coagulation-related investigations [13,14].

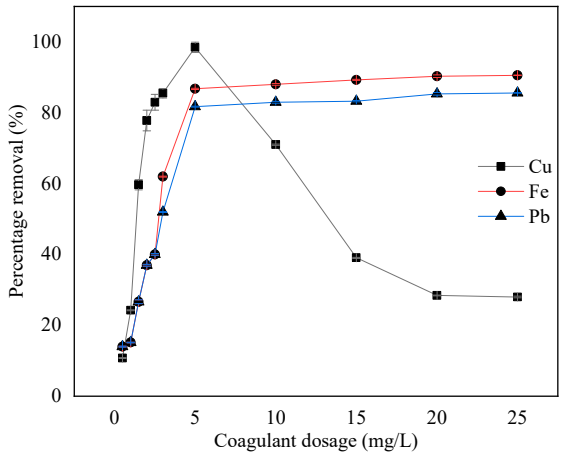

Figure 7. Effects of MCNC dosage on Cu/Pb/Fe removal from aqueous solution (initial concentration of (Cu/Pb/Fe): 20 mg/L, pH: 7.20, volume: 500 mL.

3.3. Adsorption Isotherm Results

The mechanism of the adsorption process is described by the adsorption isotherm only. This concept relates the equilibrium concentration of trace metals on the surface of MCNC (q_e) to the concentration of the Cu/Pb/Fe in the liquid (C_e) using 25 to 45 °C temperature ranges as presented in Figure 8 [34]. In general, a direct relationship between the removal efficiency of trace metals and the temperature was observed and this is an indication that high temperatures enhanced the rate of diffusion of trace metals across the surface of the MCNC [35]. Both the Langmuir and Freundlich models were fitted to the isothermic data. The Langmuir model assumes monolayer adsorption to a homogeneous surface and is given as follows:

$$\frac{C_e}{q_e} = \frac{C_e}{q_m} + \frac{1}{k_L q_m} \quad (1)$$

whereas the Freundlich adsorption model is used to explain the multilayer adsorption on the surface of an adsorbent in a non-uniform manner; the equation is given below [36]:

$$\ln q_e = \ln k_f + \frac{1}{n} \ln C_e \quad (2)$$

where:

C_e is the equilibrium concentration (mg/L);

q_e is the amount of Cu/Pb/Fe adsorbed on the MCNC at the equilibrium (mg/g);

q_m is the maximum adsorption capacity, which describes a complete monolayer adsorption (mg/g);

k_L is a Langmuir isotherm constant (L/mg) related to the free energy of adsorption; and k_F and n are the Freundlich constants.

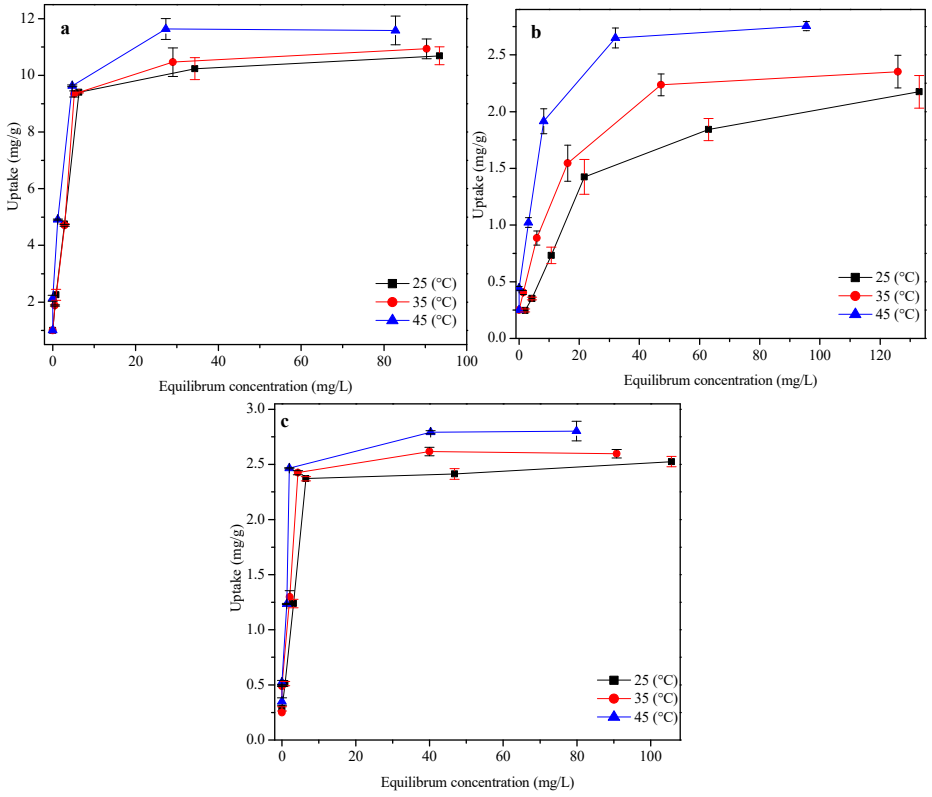

Figure 8. Effect of temperature on MCNC and equilibrium data fit to linear plots: (**a**) adsorption equilibrium isotherms of Cu; (**b**) adsorption equilibrium isotherms of Fe; (**c**) adsorption equilibrium isotherms of Pb sorption (initial concentration of (Cu/Pb/Fe): 10 to 200 mg/L, pH: 7.20, volume: 50 mL, coagulant dosage: 0.5 mg/L).

The isotherm parameters for these trace metals' adsorption were obtained using both the Langmuir and Freundlich isotherm models, as presented in Table 2. According to the Langmuir adsorption model and Freundlich adsorption model, the values of (q_m) followed the sequence: $Cu^{2+} > Fe^{2+} > Pb^{2+}$, which conforms to the performance observed in the coagulation experiment. The data obtained from the Cu and Pb adsorption fitted well with the Langmuir adsorption model from the values of the correlation coefficients, which was indicative of chemical adsorption of these metals (Cu and Pb) on to the MCNC. Surprisingly, the data obtained from Fe adsorption fitted the Freundlich isotherm model (Table 2), suggesting that the adsorption sites were uneven and non-specific [37].

Table 2. Summary of isotherm parameters for Cu/Pb/Fe adsorption onto MCNC.

Cu-Adsorption	**Langmuir Isotherm Parameters**			**Freundlich Isotherm Parameters**		
Temperature (°C)	q_m **(mg/g)**	b **(L/mg)**	R^2	K_F **(L/g)**	**1/*n***	R^2
25	107.5	2.47	0.995	20.9	0.42	0.7287
35	111.1	2.09	0.999	22.5	0.41	0.7199
45	111.1	0.72	0.999	24.2	0.39	0.7365
Pb-Adsorption	**Langmuir Isotherm Parameters**			**Freundlich Isotherm Parameters**		
Temperature (°C)	q_m **(mg/g)**	b **(L/mg)**	R^2	K_F **(L/g)**	**1/*n***	R^2
25	2.55	1.56	0.998	0.58	0.35	0.6651
35	2.62	0.54	0.999	0.64	0.41	0.6371
45	2.82	0.47	0.999	1.75	0.34	0.5596
Fe-Adsorption	**Langmuir Isotherm Parameters**			**Freundlich Isotherm Parameters**		
Temperature (°C)	q_m **(mg/g)**	b **(L/mg)**	R^2	K_F **(L/g)**	**1/*n***	R^2
25	67.11	12.3	0.9404	7.85	0.49	0.998
35	79.37	22.8	0.7725	8.08	0.53	0.999
45	81.96	17.2	0.8825	8.94	0.55	0.999

Although the adsorption coefficient is greatly consistent with the conditions that support favourable adsorption, it is suspected that dual mechanisms took part in the Fe adsorption, whereas the specific adsorption sites were consistent in the adsorption of Cu/Pb. In all cases, the Freundlich isotherm parameters K_F displayed the same trend as the temperature increased, as presented in Table 2. Similar observations were reported in related studies [38,39].

4. Conclusions

Application of efficient products in numerous water matrices is an effective way to alleviate environmental pressures from water pollution and attain sustainability. A highly efficient coagulant was successfully developed, characterized and utilized for the removal of trace metals. X-ray diffraction analysis of the coagulants revealed the presence of peaks associated with the coagulant material, and additional phases appeared after the coagulation process that were ascribed to sodium nitrite and sodium bicarbonate used for modification. The introduction of the coagulants into simulated water containing Fe, Cu and Pb showed an interplay of coagulation and adsorption processes. SEM analysis was used to study the surface morphology of the coagulants after the interaction with the metal ions. The cluster form of floccules observed in the morphology of the coagulants after interaction with Pb/Cu ions suggested that the reaction occurred at a specific homogenous site on the surface of the MCNC, whereas Fe-floccules are evenly distributed on the surface. The performance of the MCNC was affected by the solution chemistry and process variables. The mechanisms that governed the removal of Pb/Cu/Fe were investi-

gated using adsorption techniques. Experimental data obtained from the Fe adsorption conformed to the Freundlich model, indicating that the adsorption sites were uneven and less non-specific. However, the behaviour of Cu and Pb isothermic data confirmed the adsorption of these ions at a specific homogenous site on MCNC, which was an indication of chemisorption processes. Overall, the performance achieved in this study confirmed the robustness of this material in the removal of trace metals from water.

Author Contributions: Conceptualization O.A.O.; methodology, S.R.; formal analysis, L.M.; investigation, M.S.O.; Formal analysis, T.L.; writing—original draft preparation, O.A.O.; writing—review and editing, S.R., T.L. and L.M. All authors have read and agreed to the published version of the manuscript.

Funding: The first three authors acknowledge the University of Johannesburg under the Global Excellence Stature Fellowship (GES) for financial support.

Institutional Review Board Statement: Not applicable.

Informed Consent Statement: Not applicable.

Acknowledgments: The authors would like to acknowledge the University of Johannesburg under the Global Excellence Stature Fellowship (GES) for financial support and the Department of Science and Technology (DST), Republic of South Africa for the assistance in material preparation.

Conflicts of Interest: The authors declare no conflict of interest.

References

1. Shanbehzadeh, S.; Vahid Dastjerdi, M.; Hassanzadeh, A.; Kiyanizadeh, T. Heavy Metals in Water and Sediment: A Case Study of Tembi River. *J. Environ. Public Health* **2014**, *2014*, 858720. [CrossRef] [PubMed]
2. Tchounwou, P.B.; Yedjou, C.G.; Patlolla, A.K.; Sutton, D.J. Heavy metal toxicity and the environment. *Exp. Suppl.* **2012**, *101*, 133–164. [CrossRef] [PubMed]
3. Singh, R.; Gautam, N.; Mishra, A.; Gupta, R. Heavy metals and living systems: An overview. *Indian J. Pharm.* **2011**, *43*, 246–253. [CrossRef] [PubMed]
4. Li, Q.; Liu, H.; Alattar, M.; Jiang, S.; Han, J.; Ma, Y.; Jiang, C. The preferential accumulation of heavy metals in different tissues following frequent respiratory exposure to PM2.5 in rats. *Sci. Rep.* **2015**, *5*, 16936. [CrossRef] [PubMed]
5. Barbier, O.; Jacquillet, G.; Tauc, M.; Cougnon, M.; Poujeol, P. Effect of Heavy Metals on, and Handling by, the Kidney. *Nephron. Physiol.* **2005**, *99*, 105–110. [CrossRef] [PubMed]
6. Turnlund, J.R.; Jacob, R.A.; Keen, C.L.; Strain, J.; Kelley, D.S.; Domek, J.M.; Keyes, W.R.; Ensunsa, J.L.; Lykkesfeldt, J.; Coulter, J. Long-term high copper intake: Effects on indexes of copper status, antioxidant status, and immune function in young men. *Am. J. Clin. Nutr.* **2004**, *79*, 1037–1044. [CrossRef] [PubMed]
7. Taylor, A.A.; Tsuji, J.S.; Garry, M.R.; McArdle, M.E.; Goodfellow, W.L.; Adams, W.J.; Menzie, C.A. Critical Review of Exposure and Effects: Implications for Setting Regulatory Health Criteria for Ingested Copper. *Environ. Manag.* **2020**, *65*, 131–159. [CrossRef] [PubMed]
8. Council, N.R. *Drinking Water and Health: Volume 3*; The National Academies Press: Washington, DC, USA, 1980; p. 415.
9. Ferro-García, M.A.; Rivera-Utrilla, J.; Bautista-Toledo, I.; Mingorance, M.D. Removal of lead from water by activated carbons. *Carbon* **1990**, *28*, 545–552. [CrossRef]
10. Payne, M. Lead in drinking water. *CMAJ* **2008**, *179*, 253–254. [CrossRef]
11. Jaishankar, M.; Tseten, T.; Anbalagan, N.; Mathew, B.B.; Beeregowda, K.N. Toxicity, mechanism and health effects of some heavy metals. *Interdiscip. Toxicol.* **2014**, *7*, 60–72. [CrossRef]
12. UKTAG. UK Environmental Standards and Conditions (Phase 2). SR1–2007. 2008. Available online: https://www.wfduk.org/sites/default/files/Media/Environmental%20standards/Environmental%20standards%20phase%202_Final_110309.pdf (accessed on 3 March 2008).
13. Hargreaves, A.J.; Vale, P.; Whelan, J.; Alibardi, L.; Constantino, C.; Dotro, G.; Cartmell, E.; Campo, P. Coagulation–flocculation process with metal salts, synthetic polymers and biopolymers for the removal of trace metals (Cu, Pb, Ni, Zn) from municipal wastewater. *Clean Technol. Environ. Policy* **2018**, *20*, 393–402. [CrossRef]
14. Amuda, O.; Amoo, I.; Ipinmoroti, K.; Ajayi, O. Coagulation/flocculation process in the removal of trace metals present in industrial wastewater. *J. Appl. Sci. Environ. Mgt.* **2006**, *10*, 159–162. [CrossRef]
15. Teh, C.; Budiman, P.; Shak, K.; Wu, T. Recent Advancement of Coagulation-Flocculation and Its Application in Wastewater Treatment. *Ind. Eng. Chem. Res.* **2016**, *55*. [CrossRef]
16. Charerntanyarak, L. Heavy metals removal by chemical coagulation and precipitation. *Water Sci. Technol.* **1999**, *39*, 135–138. [CrossRef]

17. Kolthoff, I.M. Theory of Coprecipitation. The Formation and Properties of Crystalline Precipitates. *J. Phys. Chem.* **1932**, *36*, 860–881. [CrossRef]
18. Sun, Y.; Zhou, S.; Chiang, P.-C.; Shah, K.J. Evaluation and optimization of enhanced coagulation process: Water and energy nexus. *Water Energy Nexus* **2019**, *2*, 25–36. [CrossRef]
19. De Benedictis, C.A.; Vilella, A.; Grabrucker, A.M. The Role of Trace Metals in Alzheimer's Disease. In *Alzheimer's Disease*; Wisniewski, T., Ed.; Codon Publications Copyright: Brisbane, Australia, 2019.
20. Gibril, M.; Tesfaye, T.; Sithole, B.; Lekha, P.; Ramjugernath, D. Optimisation and enhancement of crystalline nanocellulose production by ultrasonic pretreatment of dissolving wood pulp fibres. *Cellul. Chem. Technol.* **2018**, *52*, 9–10.
21. Oyewo, O.A.; Mutesse, B.; Leswifi, T.Y.; Onyango, M.S. Highly efficient removal of nickel and cadmium from water using sawdust-derived cellulose nanocrystals. *J. Environ. Chem. Eng.* **2019**, *7*, 103251. [CrossRef]
22. Leung, A.; Hrapovic, S.; Lam, E.; Liu, Y.; Male, K.; Mahmoud, K.; Luong, J. Characteristics and Properties of Carboxylated Cellulose Nanocrystals Prepared from a Novel One-Step Procedure. *Small* **2011**, *7*, 302–305. [CrossRef]
23. Yu, X.; Tong, S.; Ge, M.-F.; Wu, L.; Zuo, J.; Cao, C.-Y.; Song, W. Adsorption of heavy metal ions from aqueous solution by carboxylated cellulose nanocrystals. *J. Environ. Sci.* **2013**, *25*, 933–943. [CrossRef]
24. Fahim, M.A. A detailed IR study of the order–disorder phase transition of $NaNO_2$. *Thermochim. Acta* **2000**, *363*, 121–127. [CrossRef]
25. Johnson, D.; Girinathannair, P.; Ohlinger, K.; Ritchie, S.; Teuber, L.; Kirby, J. Enhanced Removal of Heavy Metals in Primary Treatment Using Coagulation and Flocculation. *Water Environ. Res.* **2008**, *80*, 472. [CrossRef] [PubMed]
26. Ramos-Vargas, S.; Huirache-Acuña, R.; Guadalupe Rutiaga-Quiñones, J.; Cortés-Martínez, R. Effective lead removal from aqueous solutions using cellulose nanofibers obtained from water hyacinth. *Water Supply* **2020**, *20*, 2715–2736. [CrossRef]
27. Ahankari, S.; George, T.; Subhedar, A.; Kar, K.K. Nanocellulose as a sustainable material for water purification. *SPE Polym.* **2020**, *1*, 69–80. [CrossRef]
28. Nkalane, A.; Oyewo, O.A.; Leswifi, T.; Onyango, M.S. Application of coagulant obtained through charge reversal of sawdust-derived cellulose nanocrystals in the enhancement of water turbidity removal. *Mater. Res. Express* **2019**, *6*, 105060. [CrossRef]
29. Oyewo, O.A.; Adeniyi, A.; Sithole, B.B.; Onyango, M.S. Sawdust-Based Cellulose Nanocrystals Incorporated with ZnO Nanoparticles as Efficient Adsorption Media in the Removal of Methylene Blue Dye. *ACS Omega* **2020**, *5*, 18798–18807. [CrossRef]
30. Gong, J.; Li, J.; Xu, J.; Xiang, Z.; Mo, L. Research on cellulose nanocrystals produced from cellulose sources with various polymorphs. *RSC Adv.* **2017**, *7*, 33486–33493. [CrossRef]
31. Alizadeh-Choobari, O. Impact of aerosol number concentration on precipitation under different precipitation rates. *Meteorol. Appl.* **2018**, *25*, 596–605. [CrossRef]
32. Abdulhadi, B.; Kot, P.; Hashim, K.; Shaw, A.; Muradov, M.; Al-Khaddar, R. Continuous-flow electrocoagulation (EC) process for iron removal from water: Experimental, statistical and economic study. *Sci. Total Environ.* **2021**, *760*. [CrossRef]
33. Zhu, H.J.; Huang, Q.; Fu, S.; Zhang, X.J.; Shi, M.Y.; Liu, B. Removal of Molybdenum(VI) from Raw Water Using Nano Zero-Valent Iron Supported on Activated Carbon. *Water* **2020**, *12*, 3162. [CrossRef]
34. Holmes, L.A.; Turner, A.; Thompson, R.C. Adsorption of trace metals to plastic resin pellets in the marine environment. *Environ. Pollut.* **2012**, *160*, 42–48. [CrossRef] [PubMed]
35. Arora, R. Adsorption of Heavy Metals—A Review. *Mater. Today Proc.* **2019**, *18*, 4745–4750. [CrossRef]
36. Mantasha, I.; Hussain, S.; Ahmad, M.; Shahid, M. Two dimensional (2D) molecular frameworks for rapid and selective adsorption of hazardous aromatic dyes from aqueous phase. *Sep. Purif. Technol.* **2019**, 116413. [CrossRef]
37. Ouyang, D.; Zhuo, Y.; Hu, L.; Zeng, Q.; Hu, Y.; He, Z. Research on the Adsorption Behavior of Heavy Metal Ions by Porous Material Prepared with Silicate Tailings. *Minerals* **2019**, *9*, 291. [CrossRef]
38. Bernard, E.; Jimoh, A. Adsorption of Pb, Fe, Cu, and Zn from industrial electroplating wastewater by orange peel activated carbon. *Int. J. Eng. Appl. Sci.* **2013**, *4*, 2305–8269.
39. Agbozu, I.; Emoruwa, F. Batch adsorption of heavy metals (Cu, Pb, Fe, Cr and Cd) from aqueous solutions using coconut husk. *Afr. J. Environ. Sci. Technol.* **2014**, *8*, 239–246. [CrossRef]